JACS
JOURNAL OF THE AMERICAN CHEMICAL SOCIETY

Communication

pubs.acs.org/JACS

Shining Light on the Dark Side of Imaging: Excited State Absorption Enhancement of a Bis-styryl BODIPY Photoacoustic Contrast Agent

Mathieu Frenette,[†] Maryam Hatamimoslehabadi,[‡] Stephanie Bellinger-Buckley,[†] Samir Laoui,[‡] Jeffrey La,[‡] Seema Bag,[†] Srivalleesha Mallidi,[§] Tayyaba Hasan,[§] Brett Bouma,[§] Chandra Yelleswarapu,*[,‡] and Jonathan Rochford*[,†]

[†]Department of Chemistry and [‡]Department of Physics, University of Massachusetts Boston, 100 Morrissey Boulevard, Boston, Massachusetts 02125, United States

[§]Wellman Center for Photomedicine, Massachusetts General Hospital, 50 Blossom Street, Boston, Massachusetts 02114, United States

Supporting Information

ABSTRACT: A first approach toward understanding the targeted design of molecular photoacoustic contrast agents (MPACs) is presented. Optical and photoacoustic Z-scan spectroscopy was used to identify how nonlinear (excited-state) absorption contributes to enhancing the photoacoustic emission of the curcuminBF$_2$ and bis-styryl (MeOPh)$_2$BODIPY dyes relative to Cy3.

Combining the advantages of both ultrasound and optical imaging, photoacoustic tomography (PAT)[1−5] and photoacoustic microscopy (PAM)[6−9] are emerging as highly promising imaging alternatives. Based upon the classical photoacoustic (PA) effect, photoacoustic imaging relies upon a materials generation of acoustic waves in response to absorption of electromagnetic radiation.[10] A major advantage of PAT and PAM over their fluorescence counterparts is that the output acoustic waves are far less susceptible to scatter than optical waves, allowing for deeper penetration, which is particularly advantageous during photoacoustic tomography (PAT) in vivo.[5] However, application of both PAT and PAM is currently limited due to a lack of available contrast agents.[11] A common assumption is that any dye with a low fluorescence quantum yield will make for a suitable PA contrast agent.[12,13] In this respect, cyanine dyes have been highly studied as molecular photoacoustic contrast agents (MPACs) with metallic and polymeric nanodimensional materials also attracting much interest of late.[12,14−21] Contrary to this assumption, we aim to demonstrate how a strongly fluorescent bis-styryl (MeOPh)$_2$BODIPY dye (Φ_{fl} = 0.719; $^1\tau$ = 5.41 ns) can display an enhanced PA signal, far exceeding that of the Cy3 (Φ_{fl} = 0.025; $^1\tau$ = 0.28 ns) cyanine dye. More importantly, with respect to the future design of efficient MPACs, an excited-state sequential absorption mechanism is identified as responsible for this PA enhancement, highlighting the advantage of a long-lived S_1 excited state combined with a high quantum yield to facilitate a strong PA emission.

To aid in this study the "naked" BODIPY dye, lacking 3,5-styryl substituents, and the curcuminBF$_2$ dyes were also investigated (Figure 1). BODIPY and curcuminoid dyes are deemed excellent candidates for MPACs due to their ease of synthetic functionalization and their strong, visible, tunable absorption.

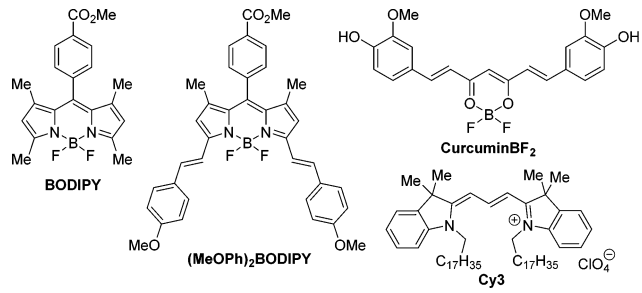

Figure 1. Molecular structures of the BODIPY, (MeOPh)$_2$BODIPY, curcuminBF$_2$, and Cy3 chromophores.

CurcuminBF$_2$ in particular was chosen due to its structural similarity to that of the bis-styryl (MeOPh)$_2$BODIPY system. Their π-conjugated styryl arms introduce the potential for a large excited-state structural volume change and PA response following photoexcitation.[22,23] Indeed, curcuminBF$_2$ has a more pronounced full width at half-maximum (fwhm = 3053 cm^{-1}) indicating a greater access to its S_1 vibrational states relative to BODIPY (fwhm = 807 cm^{-1}), hinting on a greater potential for nonradiative decay and PA response (Figure 2; Table S1, Supporting Information).

Similarly, its broad and weak fluorescence (Φ_{fl} = 0.048; $^1\tau$ = 0.72 ns) combined with the order of magnitude Stokes shift enhancement for curcuminBF$_2$ (3322 cm^{-1}) also suggests this is a more viable $S_1 \rightarrow S_0$ PA emitter relative to the rigid BODIPY system (Φ_{fl} = 0.306; $^1\tau$ = 1.98 ns; Stokes shift = 392 cm^{-1}). Introduction of the *p*-methoxy styrylbenzene substituents in the (MeOPh)$_2$BODIPY dye realizes an extended π-conjugation in both its HOMO and LUMO levels responsible for the lowest energy $S_0 \rightarrow S_1$ electronic transition (λ_{max} 640 nm; $\varepsilon = 4.34 \times 10^4$ M^{-1} cm^{-1}), similar to the curcuminBF$_2$ and Cy3 dyes (viz. DFT analysis; Figure S4, Supporting Information). However, comparable $S_0 \rightarrow S_1$ oscillator strengths and full-width at half-maxima of the BODIPY and

Received: August 21, 2014
Published: October 20, 2014

   dx.doi.org/10.1021/ja508600x | J. Am. Chem. Soc. 2014, 136, 15853−15856

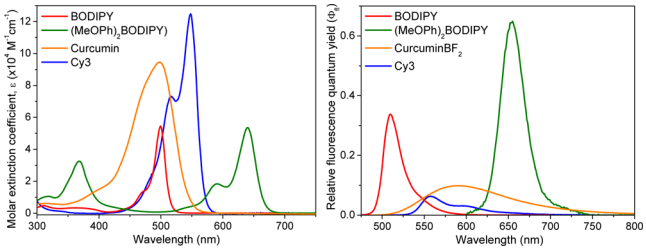

Figure 2. Electronic absorption spectra (solid) and fluorescence emission spectra (dashed) recorded in acetonitrile ($\varepsilon_{(MeOPh)2BODIPY}$ was determined in 9:1 v/v acetonitrile/dichloromethane due to poor solubility).

$(MeOPh)_2BODIPY$ dyes (fwhm = 807 and 847 cm^{-1}, respectively) indicate little divergence between their ground and excited state geometries. This observation suggests that analysis of the S_1 and S_0 electronic states alone, viz UV/vis absorption and fluorescence emission spectroscopy, is insufficient to completely explain the enhanced PA emission of $(MeOPh)_2BODIPY$.

To gain a deeper understanding of the photophysical pathway responsible for an enhanced PA emission, beyond qualitative analysis of UV/vis electronic absorption and fluorescence emission spectra, we used the optical and photoacoustic Z-scan techniques while concurrently monitoring the fluorescence signal (Scheme S1, Supporting Information).[24,25] This allows correlation of both the fluorescence and acoustic response to the linear/nonlinear optical absorption properties of each dye while incrementing the laser fluence in a controlled manner. Optical Z-scan experiments confirm a strong nonlinear (reverse saturable) absorption behavior of $(MeOPh)_2BODIPY$ consistent with sequential absorption from its longer lived S_1 excited state (Figures 3 and S6, Supporting

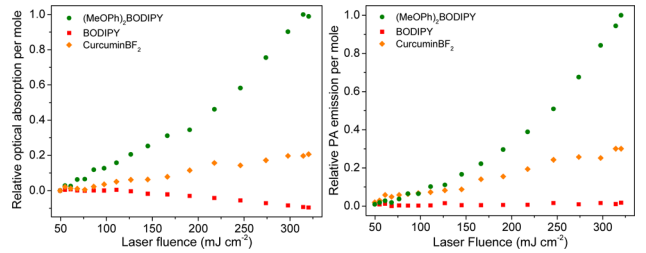

Figure 3. Relative nonlinear absorption (left) and PA emission (right) as a function of laser fluence for the BODIPY, $(MeOPh)_2BODIPY$, and $curcuminBF_2$ dyes recorded at λ_{exc} = 532 nm. For clarity, Cy3 and standard crystal violet plots are provided in the Supporting Information (Figure S7).

Information). Decisively, the strong similarity of Z-scan optical absorption and PA emission profiles for each dye unambiguously demonstrates the correlation of an enhanced PA emission with the nonlinear absorption of incident photons (Figures 3 and S7, Supporting Information).

Assuming Kashas rule[26] is still obeyed, this would imply that an $S_n \rightarrow S_1$ nonradiative decay is responsible for the observed enhancement in PA signal, followed by typical radiative versus nonradiative competition for the $S_1 \rightarrow S_0$ transition (Figures S8 and S9, Supporting Information). $CurcuminBF_2$ displays a comparable but slightly weaker nonlinear absorption and PA response, possibly due to its shorter lived excited state lifetime; however, a weaker excited state absorption coefficient (yet to be determined) may also play a role here. Contribution of sequential ground + excited state absorption (as opposed to concerted two-photon absorption) to the nonlinear optical Z-scan behavior has been confirmed by dependence of the nonlinear absorption coefficient (β) on the on-axis laser pulse intensity.[27] The excited state absorption mechanism of $(MeOPh)_2BODIPY$ and $curcuminBF_2$ was here further confirmed by the addition of 1 M 2,4-dinitrochlorobenzene (DNCB) acting as an excited-state quencher. Steady state and time-resolved fluorescence show quantitative quenching of their excited states in the presence of DNCB precluding sequential absorption of a second photon (Figure 4a) and reducing their

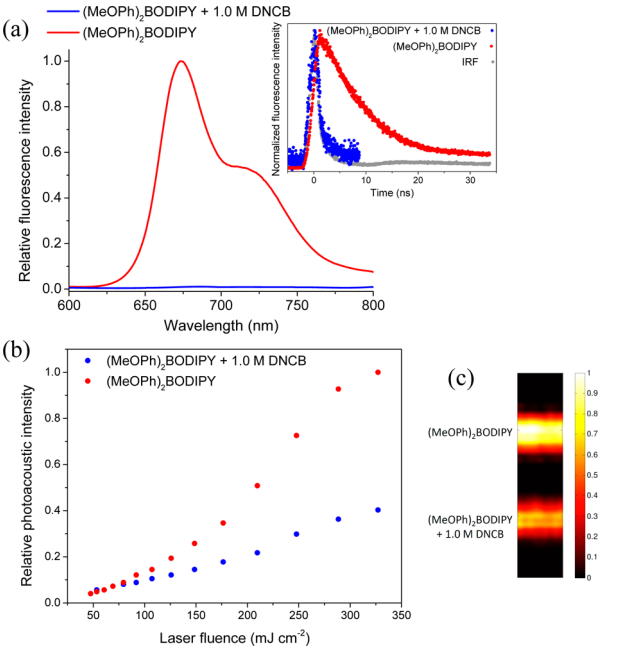

Figure 4. Quenching studies of $(MeOPh)_2BODIPY$ in 9:1 v/v acetonitrile/dichloromethane with 1 M DNCB monitored by (a) steady-state and time-resolved fluorescence, (b) PAZ-scan, and (c) photoacoustic tomography (PAT).

PA emission to that of a linear absorbing chromophore (Figure 4b) akin to the PA standard crystal violet dye. Crystal violet was identified here as an ideal PA reference due to its strong absorbance (Figure S2, Supporting Information) at the operating laser wavelength (λ_{exc} = 532 nm), rapid nonradiative relaxation ($^1\tau \approx 6$ ps),[28] linear absorption, and PA response over a wide laser fluence range (Figures S6 and S7, Supporting Information).

In comparison, the Cy3 and BODIPY dyes display saturable absorption behavior and weak PA emission (Figures S6 and S7, Supporting Information) consistent with ground state bleaching and negligible excited state absorption at 532 nm. Ultimately a true comparison of the PA response of each dye is to compare their parallel performance by photoacoustic tomography (PAT). PAT imaging at relatively high laser fluence (366 mJ cm^{-2}) shows a similar trend to PAZ-scan experiments with $(MeOPh)_2BODIPY$ and $curcuminBF_2$ showing the strongest contrast due to excited state absorption, BODIPY and Cy3 showing the poorest contrast due to ground state bleaching, and crystal violet showing an intermediate contrast due to its linear optical/photoacoustic response (Figure 5).

dx.doi.org/10.1021/ja508600x | J. Am. Chem. Soc. 2014, 136, 15853−15856

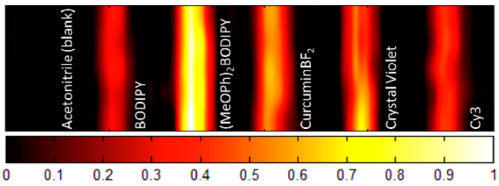

Figure 5. PAT image recorded at a laser fluence of 366 mJ cm^{-2} (λ_{exc} = 532 nm; dimension = 26.40 mm × 6.65 mm). The color scale represents the normalized acoustic intensity.

Remarkably, with a 3-fold increase in laser fluence (100 vs 300 J cm^{-2}), the excited state absorption capability of $(MeOPh)_2$BODIPY at 532 nm results in a 13-fold enhancement in PA emission. In identical conditions, curcuminBF_2 shows a reasonable 5-fold PA enhancement, whereas crystal violet, BODIPY, and Cy3 show a linear correlation to laser fluence. Considering the recommended American National Standards Institute (ANSI) maximum permissible exposure (MPE) limits of 20 mJ cm^{-2} at 532 nm, these systems are currently not applicable for nonlinear PAT in vivo imaging. However, as a proof-of-concept, they do merit future investigations in the NIR region where higher MPE limits are accessible. At low laser fluence (20 mJ cm^{-2}) excited-state absorption is minor, resulting in negligible difference between the PA contrast of each dye (Figure S16, Supporting Information). This is consistent with the identical linear absorption coefficient (α) of solutions employed for PAT experiments and the assumption of identical Gruneisan coefficient of the medium for all samples. Importantly, the use of laser fluences in the range of >100 mJ cm^{-2} is common practice for in vitro PAM applications.[29,30] The future development of efficient and biocompatible MPACs therefore holds great promise toward high resolution multiphoton PAM imaging applications.[31,32]

In conclusion, optical and photoacoustic characterization has been performed for a series of BODIPY, curcumin, cyanine, and crystal violet dyes using optical and photoacoustic Z-scan experiments. $(MeOPh)_2$BODIPY and curcuminBF_2 show promise as efficient PA emitters. BODIPY and Cy3 show weak PA emission due to ground-state bleaching, whereas crystal violet displays a linear response due to its short-lived excited state. A combination of quenching studies with standard fluorescence, optical, and PAZ-scan techniques has pointed to the role of sequential excited-state absorption followed by rapid $S_n \rightarrow S_1$ nonradiative decay as being responsible for this PA emission enhancement. On the basis of these observations, the criteria for identification and design of efficient MPACs can be redefined as requiring (i) a strong vis−NIR absorption, (ii) a long-lived S_1 excited state facilitating excited-state absorption, (iii) a large excited-state absorption extinction coefficient, and (iv) rapid $S_n \rightarrow S_1$ nonradiative decay. In essence these criteria suggest that efficient optical-limiting materials should make for desirable PA emitters. Considering the synthetic versatility and electronic tunability of both the curcumin and BODIPY class of molecules, these findings should inspire a new approach toward the future design of MPACs, particularly for PAM applications where relatively high laser fluences are accessible.

■ ASSOCIATED CONTENT

Supporting Information

Experimental methods; UV/vis spectra; computational analysis; optical, photoacoustic, and fluorescence Z-scan data; quenching experiments; photoacoustic tomography. This material is available free of charge via the Internet at http://pubs.acs.org.

■ AUTHOR INFORMATION

Corresponding Authors

*Jonathan.Rochford@umb.edu.
*Chandra.Yelleswarapu@umb.edu.

Notes

The authors declare no competing financial interest.

■ ACKNOWLEDGMENTS

The authors thank UMass Boston and Dana-Farber/Harvard Cancer Center Grant number U54CA156734 for financial support. The authors would also like to acknowledge support by NIH grants F32CA165881 (to S.M.), 5R01CA156177 (to T.H.), and S10OD012326 (to T.H.).

■ REFERENCES

(1) Ntziachristos, V.; Razansky, D. *Chem. Rev.* **2010**, *110*, 2783−2794.
(2) Mallidi, S.; Luke, G. P.; Emelianov, S. *Trends Biotechnol.* **2011**, *29*, 213−221.
(3) Xiang, L.; Wang, B.; Ji, L.; Jiang, H. *Sci. Rep.* **2013**, 3.
(4) Nie, L.; Chen, X. *Chem. Soc. Rev.* **2014**, *43*, 7132−7170.
(5) Zackrisson, S.; van de Ven, S. M. W. Y.; Gambhir, S. S. *Cancer Res.* **2014**, *74*, 979−1004.
(6) Mattison, S. P.; Applegate, B. E. *Opt. Lett.* **2014**, *39*, 4474−4477.
(7) Hai, P.; Yao, J.; Maslov, K. I.; Zhou, Y.; Wang, L. V. *Opt. Lett.* **2014**, *39*, 5192−5195.
(8) Wang, L. V.; Gao, L. *Annu. Rev. Biomed. Eng.* **2014**, *16*, 155−185.
(9) Shelton, R. L.; Applegate, B. E. *Biomed. Opt. Express* **2010**, *1*, 676−686.
(10) Bell, A. G. *Am. J. Sci.* **1880**, *20*, 305.
(11) Luke, G.; Yeager, D.; Emelianov, S. *Ann. Biomed. Eng.* **2012**, *40*, 422−437.
(12) Wang, B.; Zhao, Q.; Barkey, N. M.; Morse, D. L.; Jiang, H. *Med. Phys.* **2012**, *39*, 2512−2517.
(13) Abuteen, A.; Zanganeh, S.; Akhigbe, J.; Samankumara, L. P.; Aguirre, A.; Biswal, N.; Braune, M.; Vollertsen, A.; Roeder, B.; Brueckner, C.; Zhu, Q. *Phys. Chem. Chem. Phys.* **2013**, *15*, 18502−18509.
(14) Wang, X. D.; Ku, G.; Wegiel, M. A.; Bornhop, D. J.; Stoica, G.; Wang, L. H. V. *Opt. Lett.* **2004**, *29*, 730−732.
(15) Gao, X. H.; Cui, Y. Y.; Levenson, R. M.; Chung, L. W. K.; Nie, S. M. *Nat. Biotechnol.* **2004**, *22*, 969−976.
(16) Huang, X. H.; El-Sayed, I. H.; Qian, W.; El-Sayed, M. A. *J. Am. Chem. Soc.* **2006**, *128*, 2115−2120.
(17) Kim, C.; Song, K. H.; Gao, F.; Wang, L. V. *Radiology* **2010**, *255*, 442−450.
(18) de la Zerda, A.; Bodapati, S.; Teed, R.; May, S. Y.; Tabakman, S. M.; Liu, Z.; Khuri-Yakub, B. T.; Chen, X.; Dai, H.; Gambhir, S. S. *ACS Nano* **2012**, *6*, 4694−4701.
(19) Dykman, L.; Khlebtsov, N. *Chem. Soc. Rev.* **2012**, *41*, 2256−2282.
(20) Gutwein, L. G.; Singh, A. K.; Hahn, M. A.; Rule, M. C.; Knapik, J. A.; Moudgil, B. M.; Brown, S. C.; Grobmyer, S. R. *Int. J. Nanomed.* **2012**, *7*, 351−357.
(21) Huynh, E.; Lovell, J. F.; Helfield, B. L.; Jeon, M.; Kim, C.; Goertz, D. E.; Wilson, B. C.; Zheng, G. *J. Am. Chem. Soc.* **2012**, *134*, 16464−16467.
(22) Braslavsky, S. E.; Heibel, G. E. *Chem. Rev.* **1992**, *92*, 1381−1410.
(23) Churio, M. S.; Angermund, K. P.; Braslavsky, S. E. *J. Phys. Chem.* **1994**, *98*, 1776−1782.
(24) Sheik-Bahae, M.; Said, A. A.; Wei, T. H.; Hagan, D. J.; Van Stryland, E. W. *IEEE J. Quantum Electron.* **1990**, *26*, 760−769.
(25) Yelleswarapu, C. S.; Kothapalli, S.-R. *Opt. Express* **2010**, *18*, 9020−9025.

(26) Kasha, M. *Discuss. Faraday Soc.* **1950**, *9*, 14−19.
(27) Frenette, M.; Hatamimoslehabadi, M.; Bellinger-Buckley, S.; Laoui, S.; Bag, S.; Dantiste, O.; Rochford, J.; Yelleswarapu, C. *Chem. Phys. Lett.* **2014**, *608*, 303−307.
(28) Jessop, J. L.; Goldie, S. N.; Scranton, A. B.; Blanchard, G. J.; Rangarajan, B.; Okoroanyanwu, U.; Subramanian, R.; Templeton, M. K. *Advances in Resist Technology and Processing XVII, Proc. SPIE*; SPIE: Bellingham WA, 2000; Vol. *3999*, pp 161−170.
(29) Cook, J. R.; Frey, W.; Emelianov, S. *ACS Nano* **2013**, *7*, 1272−1280.
(30) Strohm, E. M.; Berndl, E. S. L.; Kolios, M. C. *Biophys. J.* **2013**, *105*, 59−67.
(31) Lai, Y.-H.; Lee, S.-Y.; Chang, C.-F.; Cheng, Y.-H.; Sun, C.-K. *Opt. Express* **2014**, *22*, 525−536.
(32) Shelton, R. L.; Mattison, S. P.; Applegate, B. E. *Opt. Lett.* **2014**, *39*, 3102−3105.